No. 1C-a1 $NaNbO_3$–$KNbO_3$

1b	Phase diagram: Fig. 1C-a1-001.	
3a	Lattice parameters: Fig. 1C-a1-002.	
b	Phase diagram related to subcell structures: Fig. 1C-a1-003 Subcell structures: Table 1C-a1-001, Fig. 1C-a1-004. Structural parameters: Tables 1C-a1-002...1C-a1-006; see also	75Aht
4	Thermal distortion: Fig. 1C-a1-005, Fig. 1C-a1-006.	
5a	Dielectric constant: Fig. 1C-a1-007.	
c	Remanent polarization and coercive field: Fig. 1C-a1-008.	
6a	Transition heat ΔQ_m of $(Na_{0.5}K_{0.5})NbO_3$: 85 J/mol for lower phase change and 250 J/mol for upper phase change. Transition entropy: Fig. 1C-a1-009.	54Shi2
7a	Electromechanical property: Table 1C-a1-007, Fig. 1C-a1-010, Fig. 1C-a1-011.	
	Piezoelectric properties of ceramics partially substituted by (1/3)RE for K: see	94Nar
16	Dielectric properties of thin films: see	89Tak

Table 1C-a1-001. $(Na_{0.9}K_{0.1})NbO_3$. Symmetry and tilt systems of the phases related to the transition sequence [78Aht].

Phase	Space group	Multiplicity	Transition temperature	Tilt system	*B*-cation displacement	Condensed modes
Cubic	Pm3m	$1 \times 1 \times 1$		$a^0a^0a^0$	None	
			510°C			
Tetragonal (T_2)	P4/mbm	$2 \times 2 \times 1$		$a^0a^0c^+$	None	M_3
			390°C			
Orthorhombic (F)	I2mm	$2 \times 2 \times 2$		$a^0b^+c^+$	One corner parallel	M_3, Γ_{15}
			250°C			
Orthorhombic (G)	P2mm	$2 \times 2 \times 2$		$a^-b^+c^+$	One corner parallel	M_3, R_{25}, Γ_{15}, (X)
			220°C			
Monoclinic (Q)	Pm	$2 \times 2 \times 2$		$a^-b^+c^-$	Two corner parallel	M_3, R_{25}, Γ_{15}, (X)

Table 1C-a1-002. $(Na_{1-x}K_x)NbO_3$. Lattice parameters, displacements and tilt angles in phases G, F and T_2 determined from (a) isotropic and (b) anisotropic refinements [78Aht].

	Phase G				Phase F		Phase T_2
Lattice parameters	x = 0.02		x = 0.10		x = 0.10		x = 0.10
$2 \times a_{pc}$ [Å]	7.9004(4)		7.9185(4)		7.9127(7)		7.8889(6)
$2 \times b_{pc}$ [Å]	7.8362(7)		7.8296(7)		7.8474(9)		7.8889
$2 \times c_{pc}$ [Å]	7.8376(10)		7.8418(6)		7.8666(11)		3.9443(2)
Displacements	(a)	(b)	(a)	(b)	(a)	(b)	(a/b)
Nb [Å]	0.11(1)	0.13(1)	0.12(1)	0.12(1)	0.15(1)	0.17(1)	0
Na/K [Å]	0.03(3)	0.08(3)	0.10(5)	0.04(4)	0.11(4)	0.17(52)	0
Tilt angles							
α [°]	4.6(1)	4.4(1)	2.2(2)	2.0(2)	0	0	0
β [°]	7.6(2)	5.6(5)	3.3(3)	0.5(6)	4.6(5)	2.0(9)	0
γ [°]	5.3(3)	7.2(4)	7.4(2)	7.9(1)	4.0(4)	4.2(3)	3.2(3)

Table 1C-a1-003. $(Na_{0.98}K_{0.02})NbO_3$. Atomic coordinates and temperature factors in phase G (320 °C) [78Aht]. β_{ij} is defined by Eq. (c) in Introduction.

Isotropic temperature factor refinement:

	x	*y*	*z*	*B* [Å^2]
Na/K(1)	–0.0040(31)	0	0	2.74(14)
Nb(1)	0.2636(10)	0.2541(17)	0.2435(50)	0.87(4)
O(1)	0.2270(12)	0	0.2300(3)	1.72(4)
O(5)	0.2165(10)	0.2300	1/2	1.72
O(9)	0.5	0.2270	0.2839	1.72

R_{nuc} = 12.52%, R_{prof} = 24.51%, R_{exp} = 20.44%

Anisotropic temperature factor refinement:

	x	*y*	*z*
Na/K(1)	–0.0099(32)	0	0
Nb(1)	0.2659(8)	0.2466(15)	0.2529(64)
O(1)	0.2185(19)	0	0.2307(4)
O(5)	0.2255(24)	0.2307	1/2
O(9)	0.5	0.2185	0.2745

R_{nuc} = 10.72%, R_{prof} = 23.39%, R_{exp} = 20.36%

a_{pc} = 7.9004(4) Å, b_{pc} = 7.8362(7) Å, c_{pc} = 7.9376(10) Å

	β_{11} [Å^2]	β_{22} [Å^2]	β_{33} [Å^2]	β_{12} [Å^2]	β_{13} [Å^2]	β_{23} [Å^2]
Na/K(1)	2.19(45)	5.17(102)	0.83(54)	0	0	0
Nb(1)	0.65(11)	1.72(54)	0.29(40)	–0.69(57)	0.25(58)	–0.20(25)
O(1)	1.57(34)	0.39(38)	2.33(14)	0	1.21(33)	0
O(5)	3.64(56)	2.33	0.88(43)	–2.10(37)	0	0
O(9)	1.32(19)	1.57	3.64	1.16(51)	0.32(42)	0.24(21)

$R_{nuc} = 100\ \Sigma\ |I(\text{obs}) - I(\text{calc})| / \Sigma\ I(\text{obs})$

$R_{prof} = 100\ \Sigma\ |y(\text{obs}) - y(\text{calc})| / \Sigma\ |y(\text{obs})|$

$R_{exp} = 100[(N - P) / \Sigma\ wy(\text{obs})^2]^{-1/2}$

I(obs), I(calc) = observed and calculated integrated intensity of each reflection.

y(obs), y(calc) = observed and calculated profile data point.

w = weight allotted to each data point.

Table 1C-a1-004. $(Na_{0.90}K_{0.10})NbO_3$. Atomic coordinates and temperature factors in phase F (320 °C) [78Aht].

Isotropic temperature factor refinement:

	x	*y*	*z*	*B* [Å^2]
Na/K(1)	0.014(5)	0	0	3.12(26)
Nb	0.2306(15)	0.2505(18)	0.2400(35)	0.59(11)
O(1)	0.2326(17)	0	0.25	2.12(34)
O(3)	0.2701(20)	0.25	0	2.50(40)
O(5)	0	0.2674	0.2299	2.52(21)

R_{nuc} = 16.80%, R_{prof} = 27.80%, R_{exp} = 18.73%

Anisotropic temperature factor refinement:

	x	*y*	*z*
Na/K(1)	–0.022(66)	0	0
Nb	0.2274(12)	0.2517(21)	0.2489(38)
O(1)	0.2321(15)	0	0.25
O(3)	0.2599(41)	0.25	0
O(5)	0	0.2679	0.2401

R_{nuc} = 12.07%, R_{prof} = 24.92%, R_{exp} = 18.66%

a_{pc} = 7.9127(7) Å, b_{pc} = 7.8474(9) Å, c_{pc} = 7.8666(4) Å

	β_{11} [Å^2]	β_{22} [Å^2]	β_{33} [Å^2]	β_{12} [Å^2]	β_{13} [Å^2]	β_{23} [Å^2]
Na/K(1)	4.06(93)	1.80(67)	3.05(86)	0	0	0
Nb	0.82(25)	0.70(32)	0.85(38)	0.79(39)	–0.72(58)	0.24(49)
O(1)	2.73(61)	0.21(31)	3.63(44)	0	–0.281(117)	0
O(3)	6.43(81)	3.63	0.38(44)	–0.21(147)	0	0
O(5)	0.20(32)	2.73	6.43	1.09(58)	–0.26(120)	3.63(102)

Table 1C-a1-005. $(Na_{0.90}K_{0.10})NbO_3$. Atomic coordinates and temperature factors in phase T_2 (450 °C) [78Aht].

Isotropic temperature factor refinement:

	x	*y*	*z*	*B* [Å^2]
Na/K	0	1/2	1/2	3.80(19)
Nb	0	0	0	1.76(9)
O(1)	0	0	1/2	6.58(49)
O(2)	0.2381(5)	0.7381	0	1.73(9)

R_{nuc} = 14.3%, R_{prof} = 24.6%, R_{exp} = 16.5%

Anisotropic temperature factor refinement:

	x	*y*	*z*
Na/K	0	1/2	1/2
Nb	0	0	0
O(1)	0	0	1/2
O(2)	0.2361(7)	0.7361	0

R_{nuc} = 9.7%, R_{prof} = 22.0%, R_{exp} = 16.5%
a_0 = 5.5783(4) Å, c_0 = 3.9443(2) Å

	β_{11} [Å^2]	β_{22} [Å^2]	β_{33} [Å^2]	β_{12} [Å^2]	β_{13} [Å^2]	β_{23} [Å^2]
Na/K	2.00(77)	2.00	6.30(171)	–0.19(47)	0	0
Nb	2.68(26)	2.68	–0.24(34)	0	0	0
O(1)	4.02(29)	4.02	–1.01(52)	0	0	0
O(2)	3.14(27)	3.14	4.02	0.09(41)	0	0

Table 1C-a1-006. $(Na_{0.80}K_{0.20})NbO_3$. Atomic coordinates and temperature factors in phase K (room temperature) [78Aht].

Isotropic temperature factor refinement:

	x	*y*	*z*	*B* [Å^2]
Na/K(1)	0.255(3)	0	0.232(2)	1.67(11)
Nb(1)	0.0151(5)	0.258(3)	–0.0151	0.83(4)
O(1)	–0.006(2)	0	–0.0125(15)	1.68(4)
O(5)	0.0294(3)	0.2375	1/4	1.68

R_{nuc} = 10.3%, R_{prof} = 21.7%, R_{exp} = 16.4%

Anisotropic temperature factor refinement:

	x	*y*	*z*
Na/K(1)	0.256(3)	0	0.228(2)
Nb(1)	0.0155(5)	0.252(4)	–0.0155
O(1)	–0.004(2)	0	–0.0146(14)
O(5)	0.0291(4)	0.2354	1/4

R_{nuc} = 8.6%, R_{prof} = 20.6%, R_{exp} = 16.3%

a_{pc} = 7.9162(9) Å, b_{pc} = 7.8350(4) Å, c_{pc} = 7.8993(9) Å, β = 90.325(5)°

	β_{11} [Å^2]	β_{22} [Å^2]	β_{33} [Å^2]	β_{12} [Å^2]	β_{13} [Å^2]	β_{23} [Å^2]
Na/K(1)	1.87(23)	1.10(27)	1.87	–0.53(216)	0	0
Nb(1)	0.90(9)	0.79(17)	0.90	–0.18(38)	0.03(12)	–0.50(68)
O(1)	1.83(36)	0.83(17)	2.92(44)	–1.93(45)	0	0
O(5)	2.19(17)	2.92	0.70(12)	–0.68(45)	0.20(10)	0.05(52)

Note: Standard errors in brackets do not include error in the neutron wavelength.

Table 1C-a1-007. (K,Na)NbO_3. Electromechanical characteristics of poled ceramics at RT [71Jaf].

	$K_{0.5}Na_{0.5}NbO_3$ Air-fired [a])	$K_{0.5}Na_{0.5}NbO_3$ Hot pressed [a])	(K, Na)NbO_3 [*])	$K_{0.02}Na_{0.98}NbO_3$ [b]) Air-fired
κ_{33}^{T}	290 (100 kHz)	420 (100 kHz)	$\leqq$ 450 (1 kHz)	110
Q_e (100 kHz)	≈50	≈70	$\geqq$ 20 (1 kHz)	0.7
Radial N_R [Hz m]	1650	1700	1740	1860
Dilational N_1 [Hz m]			3100	
Shear N_5 [Hz m]			1500	
ρ [Ωm]	$\approx 10^{10}$	$\approx 10^{10}$		
$1/s_{11}^{E}$ [$\cdot 10^{11}$ Nm^{-2}]	1.04	1.04	1.1	1.23
ρ_a [$\cdot 10^3$ kg m^{-3}]	4.25	4.46	$\geqq$ 4.45	
Q_{mech} (radial)	130	240	240	
Θ [°C]			195	
d_{31} [$\cdot 10^{-12}$ CN^{-1}]	32	49	49	9
d_{33} [$\cdot 10^{-12}$ CN^{-1}]	≈80	160	160	
g_{31} [$\cdot 10^{-3}$ V m N^{-1}]	12.6	13.1	14	10
g_{33} [$\cdot 10^{-3}$ V m N^{-1}]	≈31.5	43	45	
k_p	0.36	0.45	$\geqq$ 0.42	0.17
k_{31}	0.22	0.27	0.27	
k_{33}	≈0.51	0.53	0.53	
k_{15}			0.60	
P_s [$\cdot 10^{-2}$ Cm^{-2}]	22 [b])			33
P_r [$\cdot 10^{-2}$ Cm^{-2}]	18 [b])		21 [b])	33

[*]) Data are from Bausch and Lomb and are believed to refer to hot-pressed 50:50 composition.
[a]) [62Jae].
[b]) [64Dun, 65Dun].

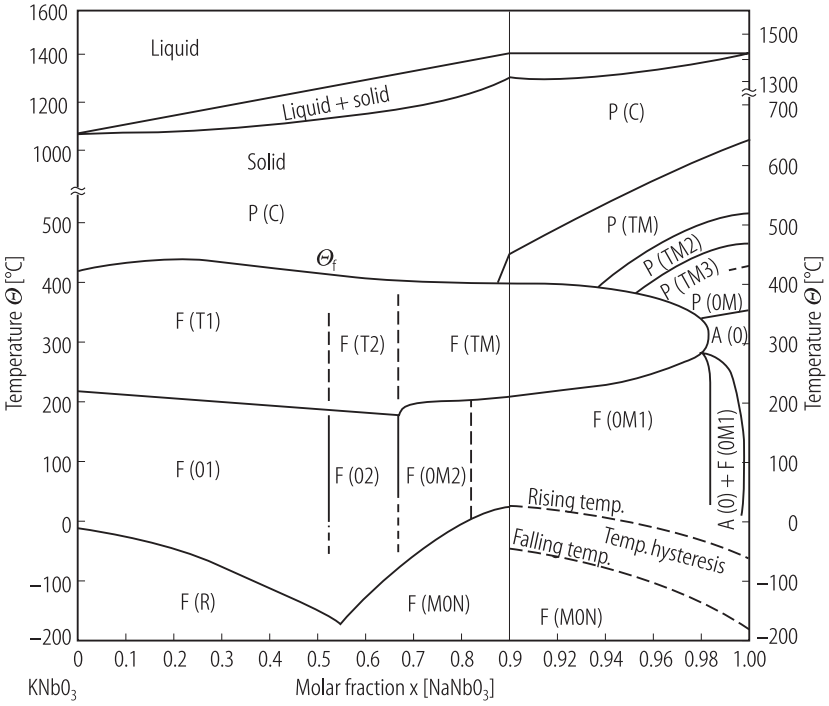

Fig. 1C-a1-001. $(K_{1-x}Na_x)NbO_3$. Phase diagram (Θ vs. x). The left side of this diagram is principally from data of [54Shi1, 59Ege] and [58Rei]. The right side is from data of [57Joh, 58Cro] and [68Ten]. Note that the temperature scale is changed for temperatures higher than 700 °C and the composition scale is changed for x larger than 0.90. P: paraelectric, F: ferroelectric, A: antiferroelectric, C: cubic, T: tetragonal, 0: orthorhombic, R: rhombohedral, MON: monoclinic and M: multiple cell.

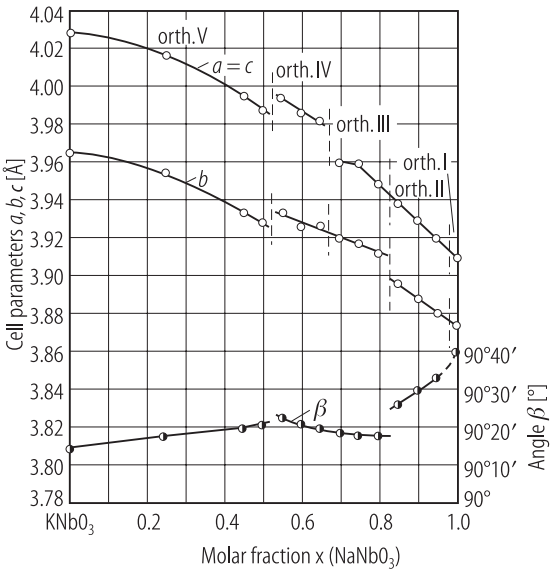

Fig. 1C-a1-002. $(K_{1-x}Na_x)NbO_3$. Perovskite-type subcell parameters vs. x [68Ten]. Pseudomonoclinic lattice parameters are used. True symmetry is indicated above the curves, where orth. means orthorhombic.

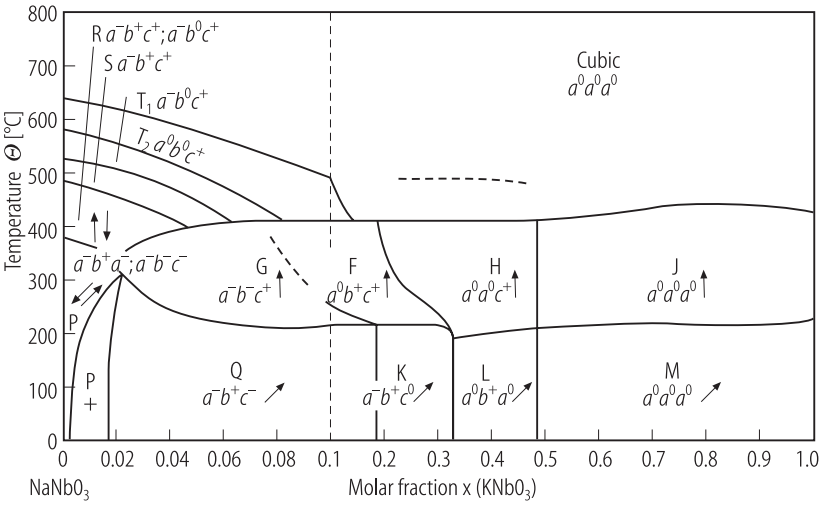

Fig. 1C-a1-003. $(Na_{1-x}K_x)NbO_3$. Phase diagram classified on the basis of subcell structures [76Aht]. The symbol, such as $a^-b^+c^-$, indicates a tilt system in the perovskite-type cell. Note change of scale at x = 0.1. See [76Aht] and [72Gla]. Vertical arrow indicates one-corner displacement, whereas oblique arrow indicates two-corner displacement.

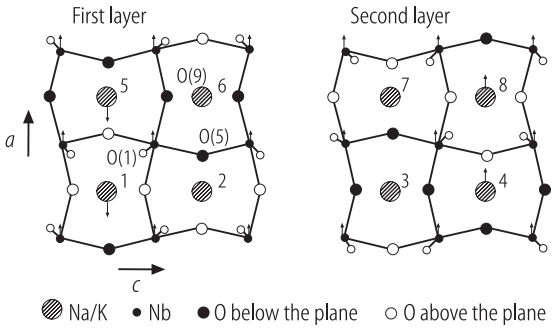

Fig. 1C-a1-004. $(Na,K)NbO_3$. Schematic picture of the atomic displacements in the phase G ($a^-b^+c^+$) to show the tilting of octahedra [78Aht].

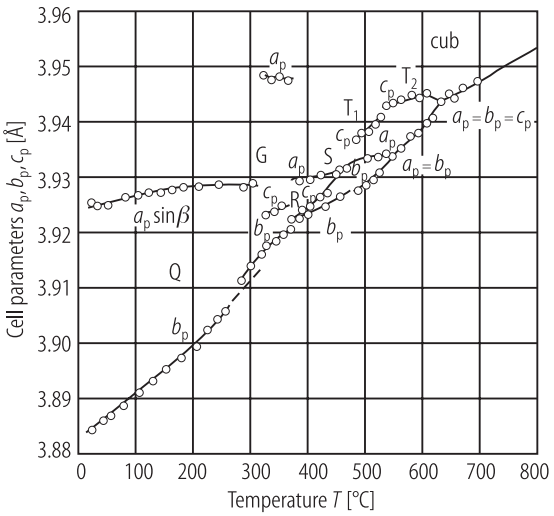

Fig. 1C-a1-005. $(Na_{0.98}K_{0.02})NbO_3$. Subcell parameters vs. *T* [76Aht]. Subscript p means pseudocubic subcell.

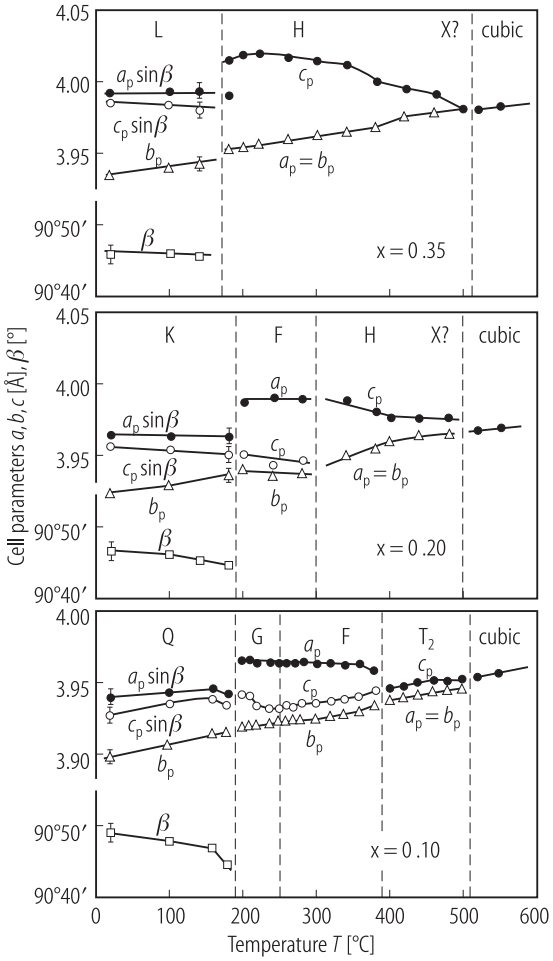

Fig. 1C-a1-006. $(Na_{1-x}K_x)NbO_3$. Subcell parameters vs. *T* [76Aht]. Parameter: x. Subscript p means pseudocubic subcell.

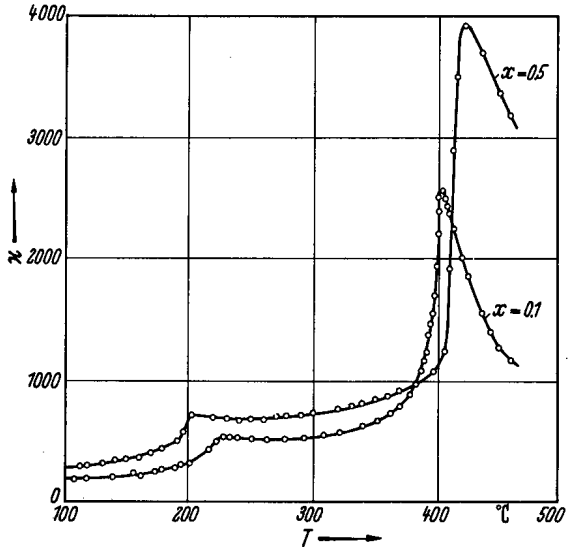

Fig. 1C-a1-007. $(Na_{1-x}K_x)NbO_3$ (ceramics). κ vs. T [54Shi2]. f = 10 kHz.

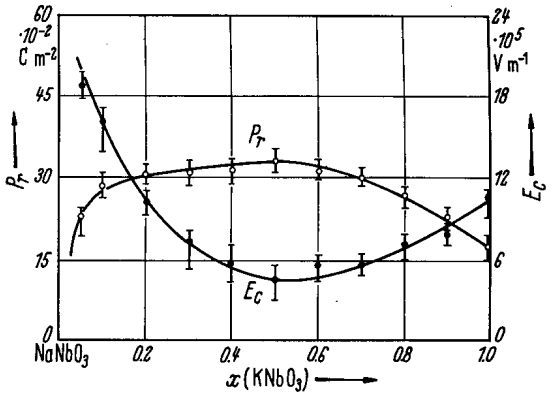

Fig. 1C-a1-008. $(Na_{1-x}K_x)NbO_3$ (ceramics). P_r and E_c vs. x [67Hae].

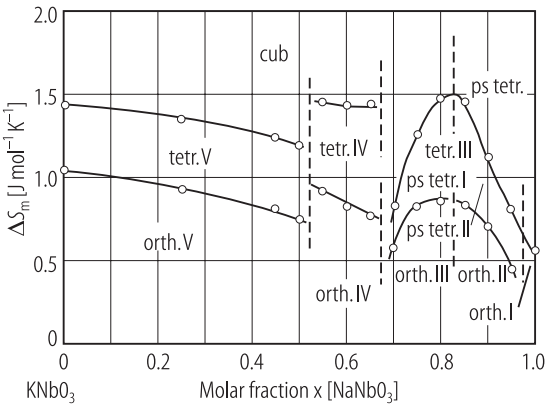

Fig. 1C-a1-009. $(K_{1-x}Na_x)NbO_3$. ΔS_m vs. x [68Ten]. ΔS_m: transition entropy. ps tetr. means pseudotetragonal. Phase line between tetr. III and ps tetr. I is not shown as the transformation was not detectable thermally.

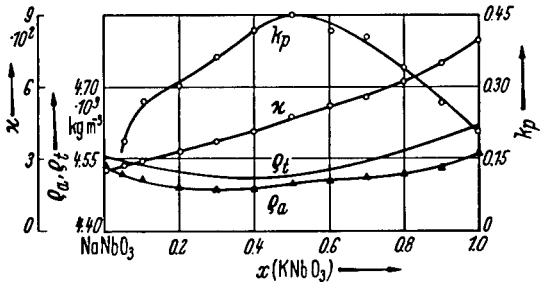

Fig. 1C-a1-010. $(Na_{1-x}K_x)NbO_3$ (ceramics). ρ_t, ρ_a, k_p and κ vs. x [67Hae]. ρ_t : true density, ρ_a: apparent density, k_p: planar electromechanical coupling coefficient, κ: dielectric constant (1 kHz).

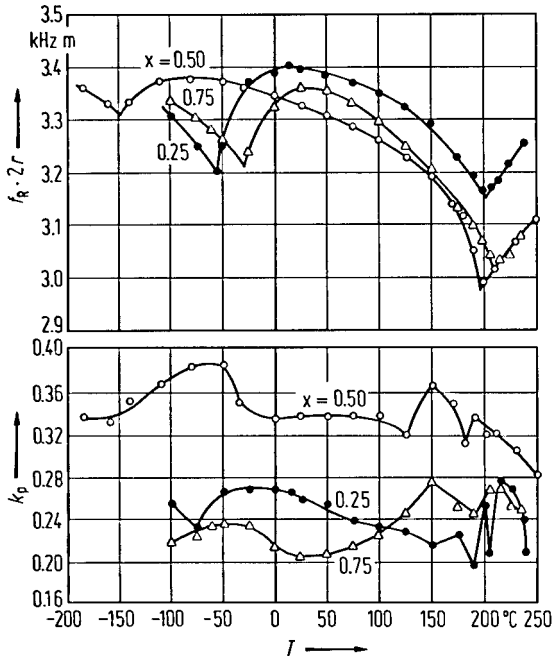

Fig. 1C-a1-011. $(K_{1-x}Na_x)NbO_3$ (ceramics). $f_R \cdot 2r$ and k_p vs. T [59Ege]. Parameter: x. $f_R \cdot 2r$: frequency constant for radial mode vibration.

References

54Shi1 Shirane, G., Danner, H., Pavlovic, A., Pepinsky, R.: Phys. Rev. **93** (1954) 672.
54Shi2 Shirane, G., Newnham, R.E., Pepinsky, R.: Phys. Rev. **96** (1954) 581.
57Joh Johns, J.F.: Master Thesis, The Pennsylvania State University, 1957.
58Cro Cross, L.E.: Nature **181** (1958) 178.
58Rei Reisman, A., Holtzberg, F., Banks, E.: J. Am. Chem. Soc. **80** (1958) 37.
59Ege Egerton, L., Dillon, D.M.: J. Am. Ceram. Soc. **42** (1959) 438.
62Jae Jaeger, R.E., Egerton, L.: J. Am. Ceram. Soc. **45** (1962) 209.
64Dun Dungan, R.H., Golding, R.D.: J. Am. Ceram. Soc. **47** (1964) 73.
65Dun Dungan, R.H., Golding, R.D.: J. Am. Ceram. Soc. **48** (1965) 601.
67Hae Haertling, C.H.: J. Am. Ceram. Soc. **50** (1967) 329.
68Ten Tennery, V.J., Hang, K.W.: J. Appl. Phys. **39** (1968) 4749.
71Jaf Jaffe, B., Cook Jr., W.R., Jaffe, H.: Piezoelectric Ceramics, London: Academic Press, 1971.
72Gla Glazer, A.M.: Acta Crystallogr., Sect. B **28** (1972) 3384.
75Aht Ahtee, M., Hewat, A.W.: Acta Crystallogr., Sect. A **31** (1975) 846.
76Aht Ahtee, M., Glazer, A.M.: Acta Crystallogr., Sect. A **32** (1976) 434.
78Aht Ahtee, M., Hewat, A.W.: Acta Crystallogr., Sect. A **34** (1978) 309.
89Tak Takahashi, K., Ueda, H., Suzuki,T., Kakegawa, K.: Ferroelectrics **95** (1989) 209.
94Nar Narayana Murty, S.: Ferroelectrics **154** (1994) 171.